

Figure 4.24: Experimental and theoretical φ^{Ey} data for horizontal CGS for specimen HomC1 for $K_I = 0.514 \text{ MPa}\sqrt{\text{m}}$ and $K_{II} = 4.4 \text{ kPa}\sqrt{\text{m}}$ with crack region masked in blue

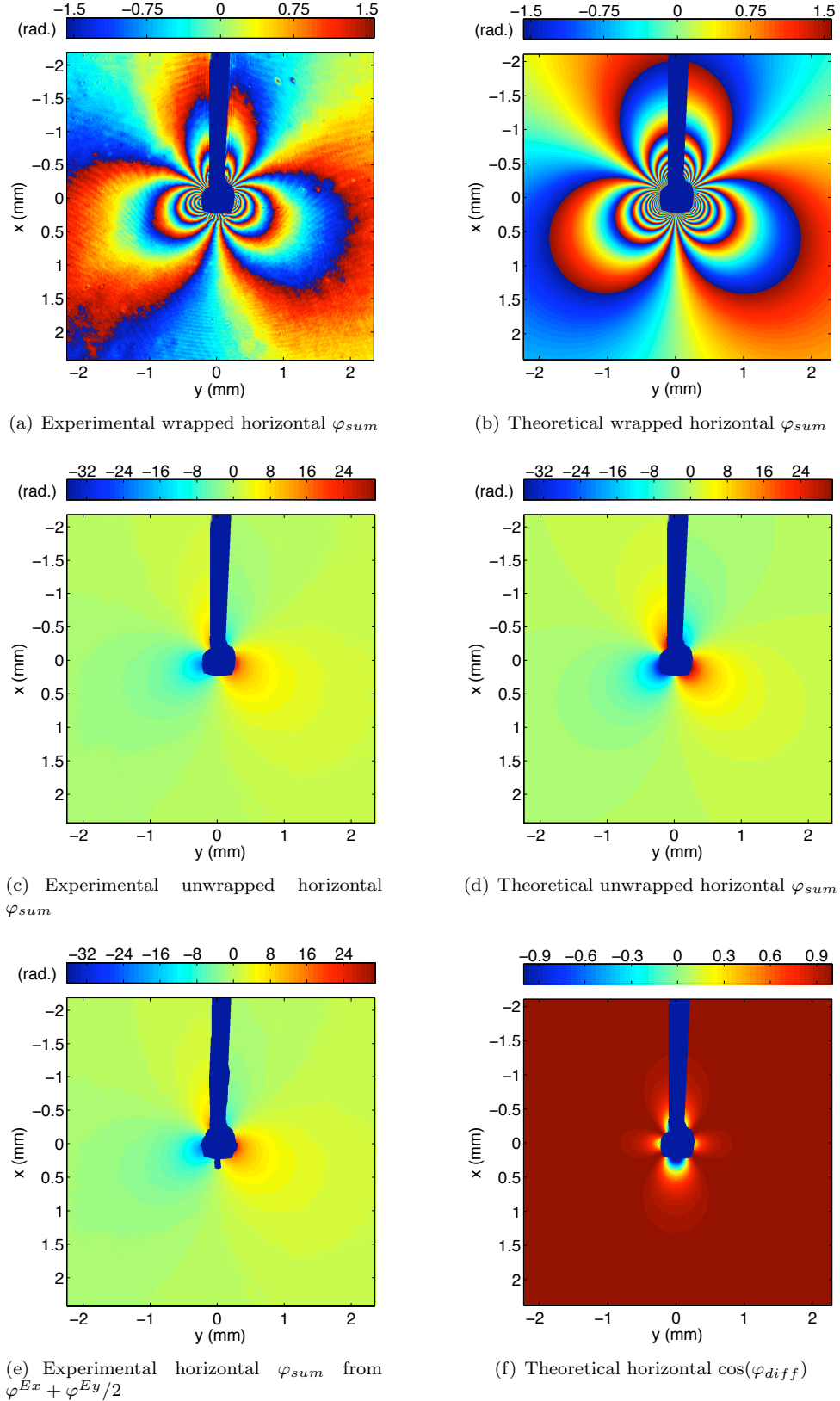


Figure 4.25: Experimental and theoretical data for horizontal CGS for specimen HomC1 for $K_I = 0.514 \text{ MPa}\sqrt{\text{m}}$ and $K_{II} = 4.4 \text{ kPa}\sqrt{\text{m}}$ with crack region masked in blue

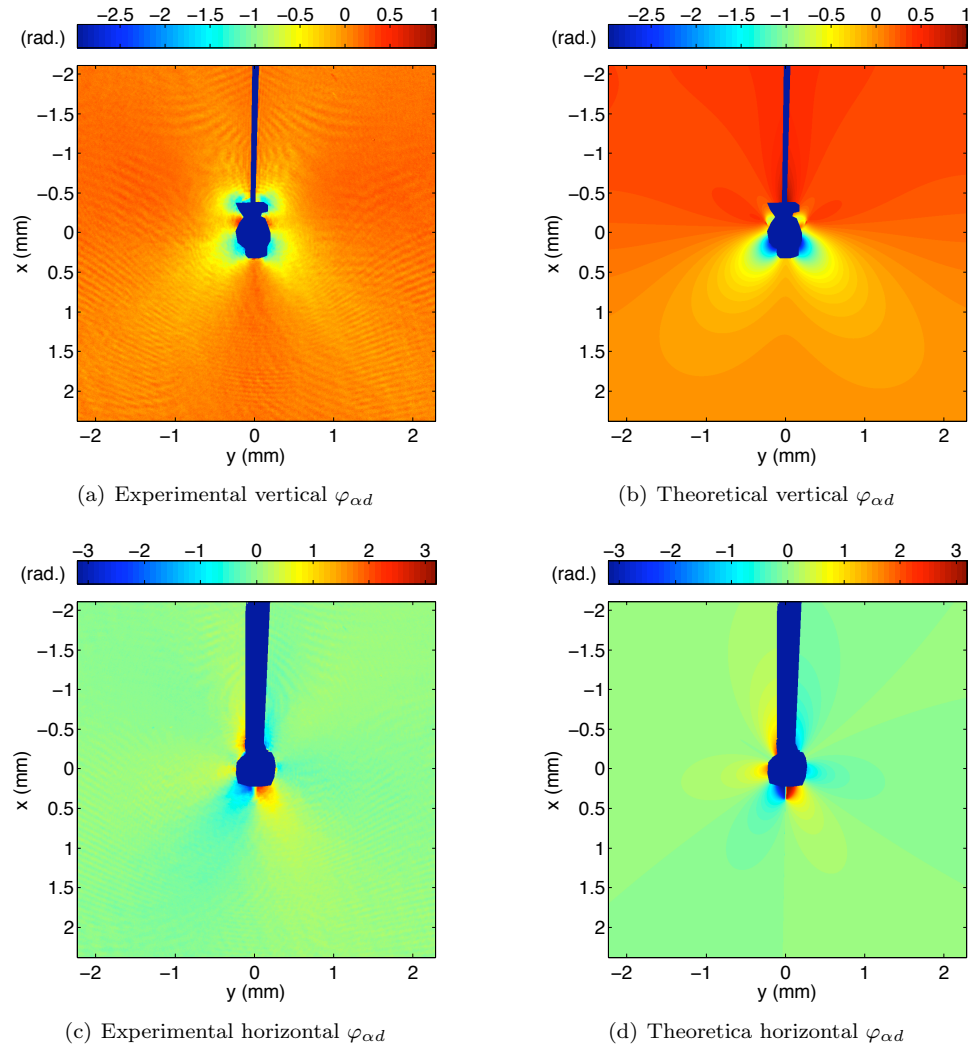


Figure 4.26: Experimental and theoretical data from vertical and horizontal CGS for the extra phase term $\varphi_{\alpha d}$ for specimen HomC1 for $K_I = 0.514 \text{ MPa}\sqrt{\text{m}}$ and $K_{II} = 4.4 \text{ kPa}\sqrt{\text{m}}$ with crack region masked in blue

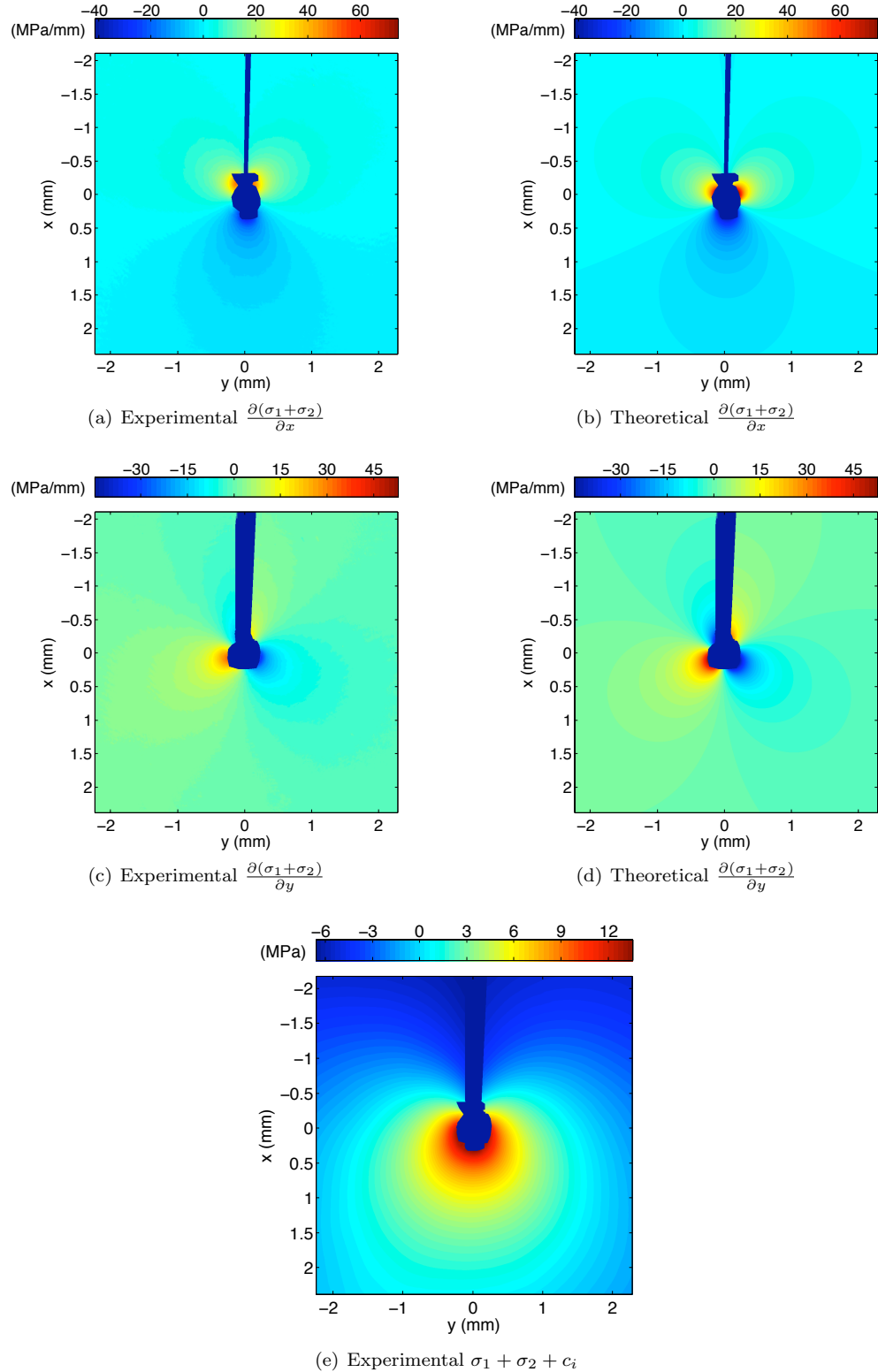


Figure 4.27: Experimental and theoretical data for the derivatives of $\sigma_1 + \sigma_2$ and the experimental integrated $\sigma_1 + \sigma_2 + c_i$ for specimen HomC1 for $K_I = 0.514 \text{ MPa}\sqrt{\text{m}}$ and $K_{II} = 4.4 \text{ kPa}\sqrt{\text{m}}$ with crack region masked in blue

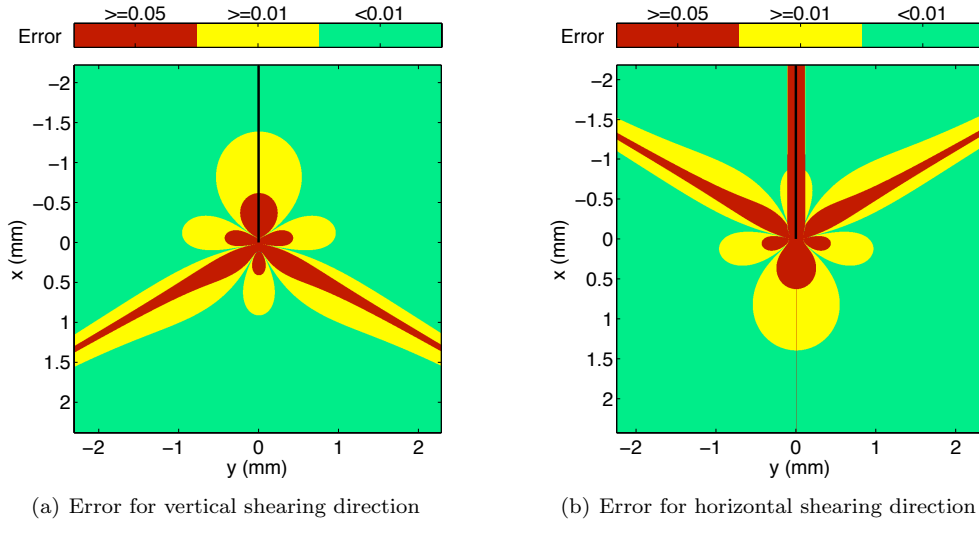


Figure 4.28: Theoretical error for CGS approximating the derivatives of $\sigma_1 + \sigma_2$, assuming K_I loading only for the 4.6 mm \times 4.6 mm field of view and lateral shearing distance of $d_{shear} = 225 \mu\text{m}$ [crack indicated in black]

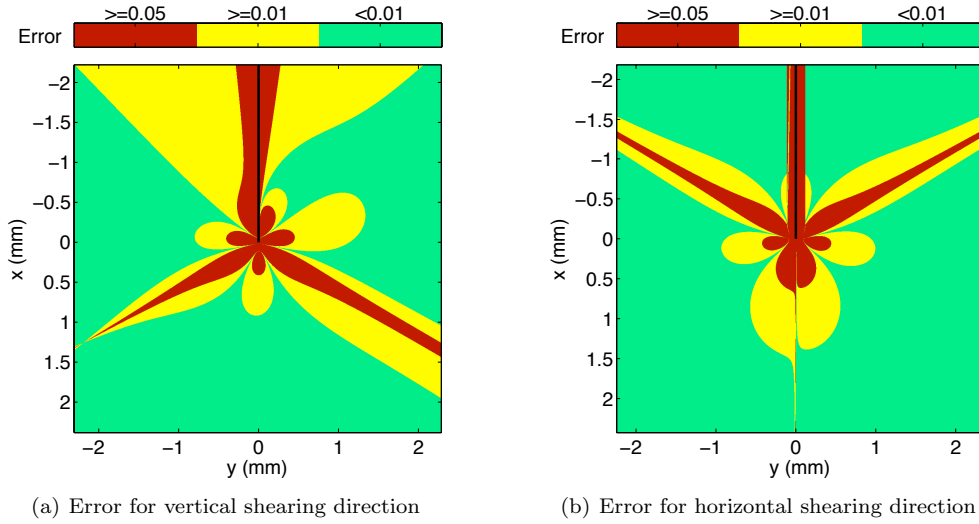


Figure 4.29: Theoretical error for CGS approximating the derivatives of $\sigma_1 + \sigma_2$, assuming $K_I = 0.514 \text{ MPa}\sqrt{\text{m}}$ and $K_{II} = 4.4 \text{ kPa}\sqrt{\text{m}}$ for the 4.6 mm \times 4.6 mm field of view and lateral shearing distance of $d_{shear} = 225 \mu\text{m}$ [crack indicated in black]